Jour. Fac. Sci., Hokkaido Univ., Ser. IV
vol. 22, no. 3, Feb., 1989, pp. 467-487.

MAGNETIC PROPERTIES OF SOME LATE PALEOZOIC TO TERTIARY SEDIMENTARY ROCKS OF TANSEN AREA, LESSER HIMALAYA, NEPAL

by

Pitambar Gautam*

(with 10 text-figures and 5 tables)

Abstract

Magnetic properties of a total number of 117 samples collected with an aim of preliminary paleomagnetic study from 26 sites in the Tansen area were investigated. Measurements of natural remanent magnetization (NRM) showed that only 11 sites (61 samples), which are represented by olive green sandstones and siltstones and redbeds (red-colored shale, sandstone and iron-rich rocks) possess magnetizations strong enough to be analyzed for stability of the remanence by alternating field (AF) and thermal (TH) demagnetization techniques. Demagnetization behavior, isothermal remanent magnetization (IRM) characteristics, X-ray diffraction patterns and variation of saturation magnetization with temperature have been studied. Chemical changes of siderite to magnetite during laboratory heating and instability of siderite-containing specimens was established. Analysis of magnetic directions obtained in the present study when combined with the paleomagnetic results on Aulis volcanics from the Tansen Group leads to recognize characteristic (probably primary), and secondary magnetizations of various ages: recent, Early Miocene, Late Eocene, Early Eocene and older.

Introduction

Rockmagnetic and paleomagnetic research on the Nepalese Lesser Himalayan rocks is still in its pioneer stage. Yoshida and Sakai (1984) made the first paleomagnetic measurements with application of AF demagnetization up to 53mT on some rocks (25 specimens from 6 sites) of probably Late Paleozoic to Eocene age in the Tansen area. They claimed that reliable paleomagnetic vectors could be determined from 4 sites after demagnetization at selected peak fields. They interpreted the bedding tilt-corrected vectors in favor of the northward drift of the Tansen area from high southern to low near-equatorial southern latitudes during the Late Paleozoic to Eocene time. A close examination of their demagnetization diagrams and the tabulated results, however, may question the actual reliability of their interpretation. In particular, the highly pronounced scatter in directions from each site, distribution of directions from some sites along great circles in stereograms or poor indications of the convergence of demagnetization paths toward the origin in the orthogonal vector-plots point out to the probable multicomponent nature of the remanence which would require more complex analysis to extract useful information. Some preliminary paleomagnetic measurements of probably Late Precambrian to Early Paleozoic sedimentary to metasedimentary

Contribution from the Department of Geology and Mineralogy, Faculty of Science, Hokkaido University, No. 1942

* On leave from the Central Department of Geology, Tribhuvan University, Kirtipur, Kathmandu, Nepal.

rocks in the vicinity of Tansen by the author showed that the rocks possessed weak magnetization intensities of about 10^{-3} to 10^{-5} A/m and were severely overprinted by viscous components of recent origin (Gautam, 1987). Some purple slates were found to possess rather strong magnetizations residing in hematite. The magnetic directions derived from the latter after thermal demagnetization were interpreted to be of secondary origin and were related to thermo-chemical effects probably associated to India-Asia collision which took place at near-equatorial latitudes, though exact mechanism of the acquisition of such component is not known. Preliminary paleomagnetic study of the volcanic rocks distributed in the Tansen area was also carried out (Gautam, 1989). Careful AF and TH demagnetization experiments of the andesite and trachyandesite rocks (33 samples from 5 sites) revealed a highly complex multicomponent magnetic remanence composed of three to four separable components, which significantly differed from one another and relative contribution to the total NRM of each of them varied even within specimens taken from one block sample. These components were interpreted as of secondary origin because of rather good grouping before any structural tilt correction and believed to have been acquired in Late Cretaceous, Early Miocene and recent times.

This work is a logical continuation of the rockmagnetic and paleomagnetic study of the Lesser Himalayan rocks in the Tansen area and deals with the magnetic properties of some sedimentary rocks and iron-rich beds from the Tansen Group, which was partly studied by Yoshida and Sakai (1984). Findings of detailed AF and TH demagnetization experiments and magnetomineralogical analyses are given. Tentative interpretation of the resolved magnetic components derived from the sedimentary rocks combined together with the results obtained from volcanics is attempted.

Geologic setting

The area studied belongs to the southern part of the Lesser Himalayan zone to the north of the Main Boundary Thrust (MBT) in the vicinity of the town of Tansen in Central West Nepal. Many scientists have contributed to the geological knowledge of this area in regional scale during the past three decades. Among the earlier works, the paper by Fuchs and Frank (1970) gives the most complete account on the stratigraphy and structure of the area which formed a part of their 'paraautochthonous Tansing unit'. Among the more recent works carried out in local scale are those by Arita and Yoshida (1982), Sakai (1983) and Hirayama et al. (1988). Sharma et al. (1984) have described the geology of the area in the context of regional geology of the Central West Nepal. A brief geological outline given here follows the Sakai's nomenclature and lithostratigraphical framework.

According to Sakai (1983), Tansen area may be divided into two major lithostratigraphic divisions: the Kali Gandaki Supergroup and the disconformably overlying Tansen Group. The Kali Gandaki Supergroup represents a sequence of non-to-weakly metamorphosed terrigenous and carbonate rocks, and is inferred to be of Late Precambrian to Early Paleozoic age. The Tansen Group, which forms the object of the present

Table 1 Lithostratigraphic description of the Tansen Group (after Sakai, 1983)

Lithostratigraphic Unit	Main Lithology	Thickness	Age
Dumri Formation	quartzose sandstone, red & green shale	725m	Oligocene to Early Miocene
— Disconformity —			
Bhainskati Formation	black shale with nummulitic limestone, hematite beds	160m	Eocene
Amile Formation	white quartzite, ferruginous quartzite, pink limestone	280m	Late Cretaceous to Paleocene
— Disconformity —			
Taltung Formation	olive green sandstone, siltstone, conglomerate and volcanics	250 to 300m	Late Jurassic to Early Cretaceous
— Disconformity —			
Sisne Formation	diamictite, slate and bioturbated mudstone	20 to 1000m	Late Carboniferous to Permian

study, consists mainly of clastic sediments and is divided into the five formations as shown in Table 1. The Tansen Group is thus believed to have an age range from Late Carboniferous to Early Miocene.

Hirayama et al. (1988) also recognize two major lithostratigraphic divisions in the Tansen area: the Nawakot Group (roughly equivalent of the Sakai's Kali Gandaki Supergroup, lithologically), consisting 'largely of pelitic, psammitic and carbonatic metasediments' and the overlying Tansen Group which is composed 'mainly of pelitic and psammitic sediments with Paleogene fossils and ferruginous sediments'. They subdivide the Tansen Group into two formations, viz. the Bhainskati Formation and the Dumre Formation (Sakai's Dumri Formation) which overlies the former. They further recognize three subdivisions within the Bhainskati Formation which are named as the Lower Pebbly Mudstone Member, the Middle Quartzite Member and the Upper Fossiliferous Shale Member. Lithologically, these members from bottom to top seem to correspond to the Sisne Formation, the Taltung and Amile Formations taken together and the Bhainskati Formation of Sakai, respectively. The major difference between the works by Hirayama et al. and Sakai, however, lies in assigning the age to these groups. Hirayama et al. assign mainly Eocene or Paleogene age to their Tansen Group and Precambrian age to the Nawakot Group. In addition, they found no positive evidence on a disconformity between Dumre and Bhainskati Formations. Their geology, however, is based on their observations limited to the central part of the Tansen area covered by Sakai (1983).

Tansen Group is folded in a large synclinorium, whose central part is occupied by a klippe derived from the underlying Kali Gandaki Supergroup. Most of the workers in the area describe that the Tansen area is characterized by complex tectonism represented by superposition of folds of several wavelengths, thrusts and faults of both longitudinal and transverse nature. The southern flank of the Tansen synclinorium exhibits an imbricate structure owing to the combination of folds and longitudinal

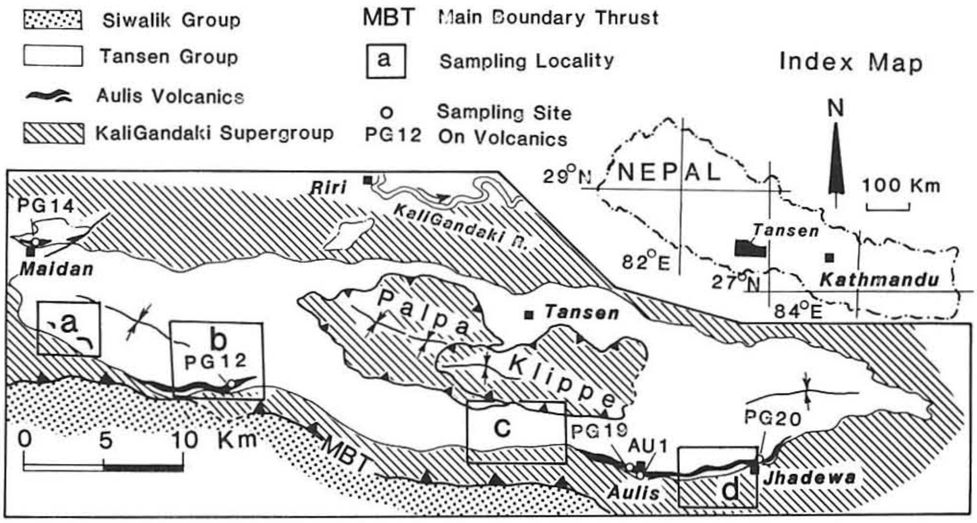

Text-fig. 1 Sampling localities (quadrangles, details in Text-fig. 2) and the schematic lithostratigraphic divisions of the Tansen area (after Sakai, 1983). Sampling localities of the Aulis Volcanics studied paleomagnetically are also shown.

reverse faults.

A geologic sketch map of the area is shown in Text-fig. 1.

Sampling and laboratory procedure

Oriented block samples were taken from all sites except site Ta10. Samples from site Ta10 and part of the collection from site Dm06 consisted of cores of 2.54cm diameter directly drilled *in situ* by the aid of a gasoline-powered portable driller. Sampling sites are distributed in four locations. Sampling of these rocks and the volcanic rocks, which were studied separately, was accomplished simultaneously. Particular attention was paid to sampling of red beds and fine-grained clastic sediments because of their proven suitability for magnetic studies. Sampling localities are shown in Text-fig. 1 and the sampling sites in each area are shown in Text-fig. 2. Further sampling details are given in Table 2.

In the laboratory, specimens in the form of cylinders (2.54cm in diameter and 2.4cm in length) were cut and the measurements of their remanent magnetism were made on a Schonstedt spinner magnetometer (Model SSM-1A) coupled with a Sord M-100 microcomputer system which calculates resultant magnetic directions, specimen intensities, and standard deviations. Stepwise AF demagnetization of specimens was carried out on a 400-Hz AF demagnetizer capable of producing a maximum field of 53mT. Five or 10mT steps were employed. Progressive TH demagnetization was performed by heating the specimens in air inside a non-inductive furnace with steps mostly in the range between 25 to 100°C from room temperature to a maximum of 670°C.

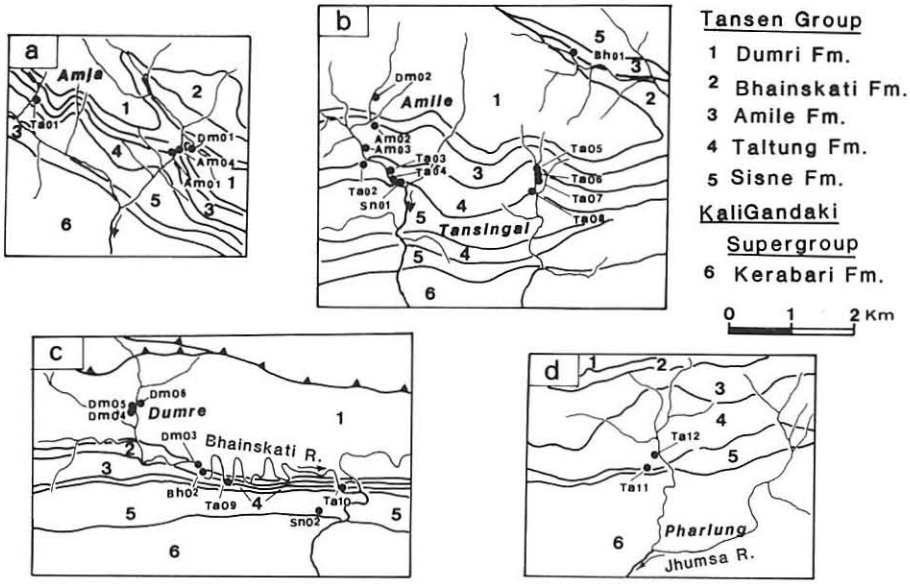

Text-fig. 2 Distribution of sampling sites in Amja, Amile-Tansingal, Dumre and Pharlung areas. Formation nomenclature and the boundaries are according to that of Sakai (1983).

Demagnetization coil and the furnace (during heating and cooling cycles) were placed inside a reasonably field-free space created by system of pairs of Helmholtz coils which compensated the ambient geomagnetic field in the laboratory.

Thermomagnetic analysis was carried out on whole-rock (Chip) samples by means of a vertical balance equipped with automatic recording system. The samples were cycled from room temperature up to 630°C and back in air-free space (Vacuum close to 0.26 Pa.) with heating-cooling rate of 10°C/min. X-ray analysis on powdered specimens was carried out to determine the main mineral phases present in fresh or heated sediments by using an X-ray diffractometer with Cu Kα radiation. A scanning speed of 1°/minute and a time constant of normally 2 seconds were employed. An IRM in fields to about 0.4 T was imparted to several specimens already subjected to demagnetization using an electromagnet with an aim to identify the magnetic phases (magnetite or hematite) on the basis of their hardness in coercivity spectra (Dunlop, 1972). All the measurements were carried out at the paleomagnetic laboratory of Hokkaido University.

NRM measurements and demagnetization studies

Natural remanent magnetization (NRM) data

Site-mean NRM intensities at specimen level ranged from 0.8×10^{-4} A m^{-1} to $4{,}905 \times 10^{-4}$ A m^{-1} (Table 2). Coarse-grained sandstones, black slates, gray shales

Table 2 Natural remanent magnetization intensities and directions with sampling details

Site	N (n)	Intensity (× 10^{-4} A/m)		Mean Direction				Lithology	Attitude
		Mean	±S	D (deg.)	I (deg.)	k	α_{95} (deg.)		Strike/Dip
Dumri Formation:									
Dm01	6 (4)	12.6	± 13.3	188	36	2	38.0	light gray ss.	310 /60 N
Dm02	3 (3)	50.4	± 84.5	314	8	6	34.2	pink ss.	315 /90 N
Dm03	7 (4)	7.1	± 5.5	352	12	1	48.1	light gray ss.	285 /85 N
Dm04	13 (4)	208.3	± 115.2	75	−57	161	3.0	purple slt.	265 /80 N
Dm05	6 (5)	46.8	± 79.2	84	−83	1	53.8	light gray ss.	265 /80 N
Dm06	16 (8)	132.3	± 38.6	65	−51	124	3.1	purple silty sh.	272 /88 N
Bhainskati Formation:									
Bh01	12 (6)	4,905.0	±1351.0	356	37	133	3.5	sil. ironstone	254 /48 N
Bh02	22 (12)	319.2	± 192.6	348	46	8	10.4	hematitic ss.	300 /68 N
Amile Formation:									
Am01	3 (2)	3.9	± 2.5	358	48	24	16.5	gray ss.	305 /30 N
Am02	22 (6)	18.6	± 16.4	027	46	16	7.5	reddish brown ss.	282 /74 N
Am03	19 (7)	89.5	± 31.8	230	−78	160	2.5	calc. purple ss.	275 /78 N
Am04	7 (3)	65.8	± 28.5	001	40	269	3.2	hematitic ss.	305 /25 N
Taltung Formation:									
Ta01	14 (5)	4.7	± 4.0	356	29	2	23.7	black carb. slt.	310 /45 N
Ta02	9 (4)	272.7	± 136.2	355	−55	80	5.2	dark brown ss.	295 /50 N
Ta03	9 (3)	13.3	± 10.5	167	−28	1	45.8	gray ss.	295 /50 N
Ta04	12 (4)	6.1	± 2.5	355	−19	7	15.8	olive green ss.	270 /55 N
Ta05	16 (5)	342.7	± 176.4	330	−61	27	6.7	hematitic and sideritic ss.	260 /40 N
Ta06	11 (4)	23.7	± 20.4	336	5	2	33.3	gray calc. ss.	258 /32 N
Ta07	15 (6)	27.3	± 14.5	342	− 9	2	27.8	olive green ss.	260 /30 N
Ta08	8 (3)	0.8	± 0.5	007	77	2	38.0	gray ss.	240 /35 N
Ta09	10 (4)	73.6	± 21.6	353	55	15	11.3	gray calc. ss.	265/124 N
Ta10	4 (4)	67.7	± 20.8	028	43	34	11.9	olive green ss.	275/110 N
Ta11	6 (3)	19.9	± 7.3	003	41	21	12.6	congl. ss.	235 /45 N
Ta12	5 (4)	33.6	± 30.2	325	5	3	34.9	congl. ss.	235 /45 N
Sisne Formation:									
Sn01	2 (1)	23.7	± 20.4	174	39	-	-	gray shale	288 /58 N
Sn02	9 (3)	2.6	± 1.0	357	45	5	21.7	diamictite	-

Note: — N: no. of specimens; n: no. of samples; S: standard deviation of mean intensity; D: declination; I: inclination; k: estimate of the precision parameter; α_{95}: radius of 95% confidence circle. Mean directions and the statistical parameters are calculated using Fisherian statistics giving unit weight to specimens. Directions are in **situ.** ss. = sandstone, slt. = siltstone, sil. = siliceous, cal. = calcareous, carb. = carbonaceous, and congl. = conglomeratic.

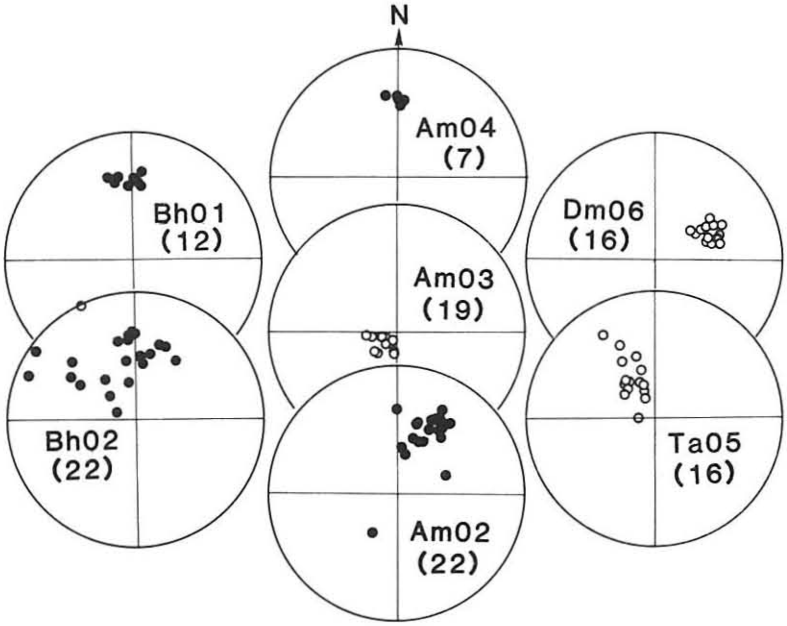

Text-fig. 3 Equal-area (Schmidt's net) plots to show the pronounced grouping of specimen NRM directions (*in situ*) from some redbed sites. Number of specimens from each site is given. Solid and open circles indicate positive and negative inclinations, respectively.

and diamictites had very weak magnetic moments and highly scattered magnetic directions. Redbeds, in contrast, possessed strong NRM intensities and exhibited rather well-grouped magnetic directions. Text-fig. 3 demonstrates equal-area projections of specimen directions for some red bed sites. It can be observed that these sites are dominated by specific components of diverse orientation. Site Ta02 is also characterized by well-concentrated specimen NRM directions.

Alternating field demagnetization results

AF demagnetization of some weakly magnetized samples (e.g., black slates, diamictite, light colored sandstones) showed rapid decay of the initial intensities at few initial demagnetization steps and yielded random directions. Redbeds, in contrast, were extremely hard to AF treatments up to 53mT. They exhibited less than 5% changes in initial intensity and occasionally changes in directions of a few degrees. The only specimens which effectively responded to AF cleaning are from the Taltung Formation (Sites Ta02, Ta04, Ta07, Ta09 and Ta10) with essentially olive-green siltstone and sandstone lithologies which contain volcanic detritus. Their widely varying responses to demagnetization are displayed in Text-fig. 4. For example, specimens from site Ta07 show progressive changes in directions in successive demagnetization steps leading to better grouping due to effective removal of softer component. However, specimens from site Ta02 show only minor changes to such treatment probably due to lesser contribution of the softer somponent(s) to the initial magnetic remanence. Because of such non-unique demagnetization behavior, all specimens were step-demagnetized and a complex analysis was undertaken to resolve the multicomponent remanence.

Visual analysis of the demagnetization data in the first step included recognition of linear segments in the vector-plots (Zijderveld, 1967) and search for great circle trends (converging remagnetization circles) in the vector migration plots. The second step, then, was linearity spectrum analysis to separate the collinear data-point segments (Schmidt, 1982) followed by subsequent least-square line fitting to the data-points (Kirschvink, 1980) and remagnetization circle pole analysis by the method of Bailey

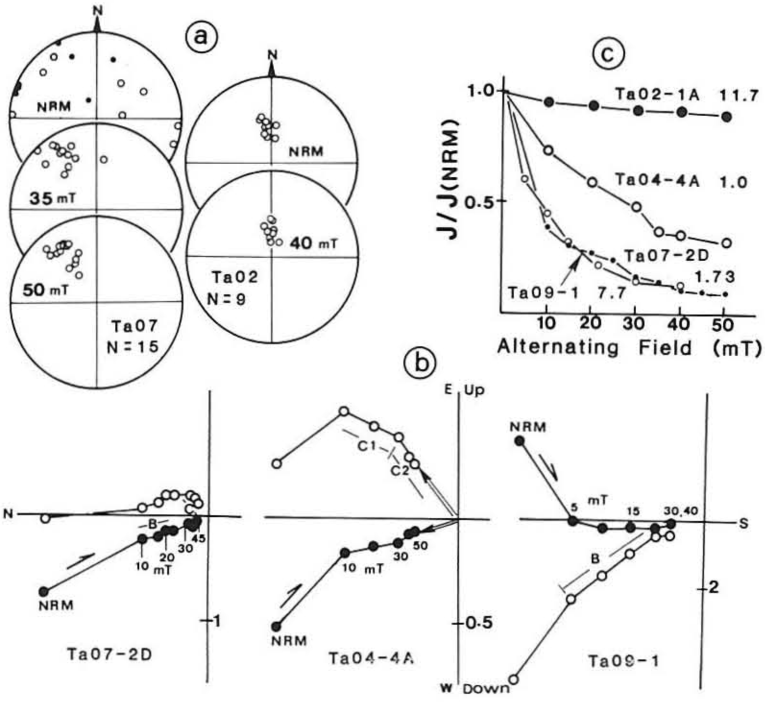

Text-fig. 4 Results of stepwise AF demagnetization (before tilt corrections) for some non-red specimens from the Taltung Formation.

a. Progression of grouping in specimen directions from sites Ta07 (left) and Ta02 (right) at selected peak fields.

b. Orthogonal projection diagrams (Zijderveld, 1967).

Projections of the end-points of the resultant magnetic vector during successive demagnetization. Solid and open circles represent the projections on the horizontal and north-south vertical planes respectively. Units along axes are given in mA/m. Numbers besides solid circles refer to peak alternating field (only selected values are shown). Symbols designating the components reflected in the linear segments (B, C1, C2) are also shown.

c. Normalized intensity response curves. Numerical value following the specimen name denotes the magnitude of initial NRM intensity, J (NRM), in mA/m.

and Halls (1984). In practice, the linearity coefficients for meaningful segments were around 0.99 and they were accepted as reliable estimates if the best-fit line had the maximum angular deviation less than 10°. In addition, well-grouped mean direction at certain peak field was assumed as reliable estimate of the stable direction. The results of analysis are presented in Table 3. As all the components have nearly northerly declinations, discrimination of the components had to be based on inclination values: Directions with positive inclinations close to that of the present dipole field at the study area (I = 47°) are designated as A. Those having significantly shallower but positive inclinations are termed as B. Component C has moderately upward inclinations. Samples with component A as the only dominant one from some sites (e.g. Sn02, Ta11) are not considered here.

Table 3 Results of alternating field demagnetization

Site	N_u (N_t)[1]	Method[2]	AF value or range[3]	Mean Direction[4] D (deg.)	I (deg.)	k	α_{95} (deg.)	Component designation
Ta02	9 (9)	Peak AF	40 mT	359	−65	79	5.2	C2
Ta04	7 (12)	LSA/LSQ	10-20 mT	345	35	12	14.9	B
	4 (12)	LSA/LSQ	<40 mT	346	−25	27	13.5	C1
	12 (12)	Peak AF	40 mT	340	−54	35	6.8	C2
	12 (12)	CRC	10-20 mT	352	−54	95	(5.3-13.0)	C2
Ta07	8 (14)	LSA/LSQ	<40 mT	333	27	110	4.7	B
	14 (14)	Peak AF	50 mT	328	−32	34	6.4	C2
	12 (14)	CRC	<50 mT	332	−33	160	(4.2-9.1)	C2
Ta09	4 (4)	LSA/LSQ	<20 mT	356	47	36	11.7	A
	4 (4)	Peak AF	20 mT	350	24	81	7.8	B
Ta10	4 (4)	LSA/LSQ	<20 mT	020	46	76	8.1	A
	4 (4)	Peak AF	20 mT	006	23	118	6.4	B

Note: — 1. N_u and N_t are the number of specimens in which the corresponding direction could be identified and the total number of specimens demagnetized, respectively.

2. LSA: linearity spectrum analysis, LSQ: least-square line analysis, CRC: converging remagnetization circle analysis, AF: alternating field.

3. In some cases, only the upper limit is given because the lower limit varied from specimen to specimen.

4. Mean directions are **in situ**. Parameters are calculated giving unit weight to each of the N_u and have same meaning as in Table 2 except for CRC pole data. For the latter estimates, the minimum error and maximum error radii at 95% confidence level are given.

Thermal demagnetization results

Altogether eleven specimens (one each from sites Dm04, Dm06, Bh01, Am02, Am03, Am04 and Ta02 but two each from sites Bh02 and Ta05 due to lithologic differences in the latter) were thermally demagnetized during pilot experiments. Such experiments led to recognize two groups of specimens based on the consistency in the directional changes and degree of chemical alteration effects.

First group specimens maintain high directional stability or consistent directional patterns up to peak temperatures of 550—625°C or above before components caused by chemical alterations or build-up of viscous noise begin to randomize the NRM. Text-fig. 5 displays a wide variety of specimen responses owing to components of diverse origin and unblocking temperatures. Specimens from Dumri Formation (e.g. specimen Dm06-4B) show high directional stability up to 650—670°C with unblocking temperatures distributed above 350°C. The survival of directions up to such higher temperatures indicate that hematite is the prominent carrier of the remanence. Minor chemical changes were noticed around 525°C but they did not change the directions. Specimens from Bh01 and part of specimens from Bh02 maintain directional stability up to 550—600°C but chemical changes start before the intensity becomes reduced to about half of the initial value. Part of the intensity loss is observed below 300°C with a marked decrease between 200 and 300°C. Unblocking temperatures are rather thermally distributed. Specimens from Am03 and some specimens from Ta05 indicate two-

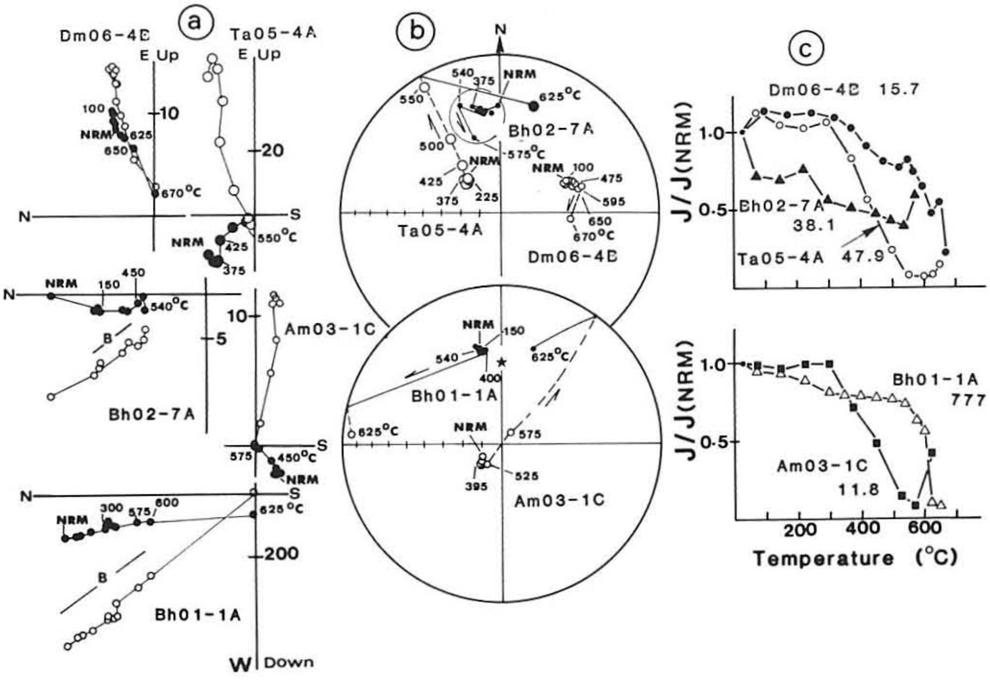

Text-fig. 5 Thermal demagnetization results (before tilt corrections) for selected redbed specimens (Dm06-4B, Bh01-1A, Bh02-7A, Am03-1C and Ta05-4A).

a. Orthogonal projection diagrams. Numbers refer to the selected peak temperatures. Some data-points at final steps thought to be affected by chemical changes are not shown.

b. Vector migration plots (equal-area net) showing directional changes of the remanent magnetic vector during successive demagnetization by heating. For clarity, only selected temperatures are indicated. Star is the dipole field direction (I = 47°) at Tansen.

c. Normalized intensity response curves. J (NRM) values, in mA/m, are given after the specimen name. Other symbols as in Text-fig. 4.

component nature. The resultant magnetization vectors tend to follow great circle trends converging towards moderately downward inclined northerly directions probably close to either component A or B though the convergence could not be established due to random nature at high temperatures. A distinct feature for these specimens is about 80—90% unblocking of the total intensity linearly between 275 to 575°C.

Second group specimens acquire large random components due to production of an unstable intergrown material (probably magnetite or maghemite owing to very high intensities) as a result of mineralogical change during heating. Such changes start at temperatures as low as 75°C. Intensity responses are illustrated in Text-fig. 6. Whatever the cause of such dramatic changes in intensity (note that a logarithmic scale is used for the ordinate), it is clear that no meaningful paleodirections can be extracted from such specimens. Samples with stable characteristics were further studied by mass demagnetization at selected peak temperatures. Meaningful results are summarized in Table 4. Specimen from site Ta02 showed random behavior due to chemical alterations and so was not considered further.

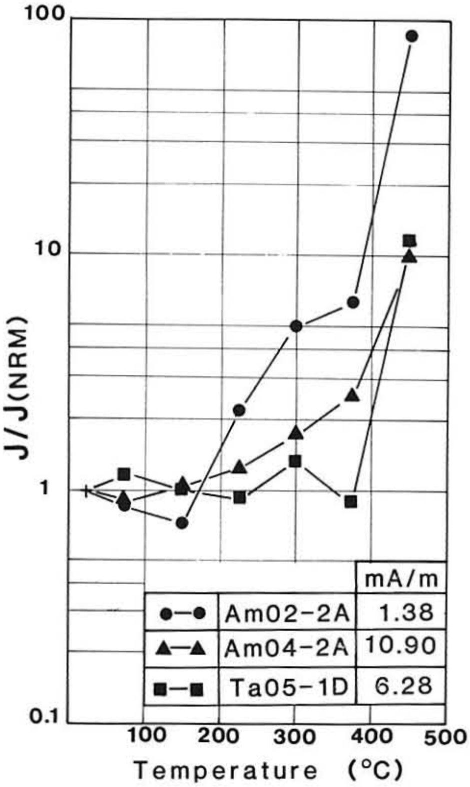

Text-fig. 6 Normalized intensity response curves for some selected specimens (Am02-2A, Am04-2A and Ta05-1D) which showed dramatic intensity changes due to chemical changes during heating. Values in mA/m are J (NRM) magnitudes.

Table 4 Results of thermal demagnetization

Site	n	cleaning temperature (deg. C)	Mean Direction D (deg.)	I (deg.)	k	α_{95} (deg.)	Component designation
Dm04	4	500	077	−59	203	4.9	characteristic
Dm06	8	500	062	−48	186	3.7	characteristic
Bh02	8	500	352	40	29	9.3	B
Am03	7	400	219	−78	181	3.9	characteristic
Am04	3	300	008	36	421	3.9	B
Ta05	5	300	321	−64	46	9.3	unresolved

n denotes the number of samples. Statistical parameters are calculated giving unit weight to samples. All directions are **in situ**.

Magnetomineralogy

Thermomagnetic analysis

Thermomagnetic analysis was attempted for specimens having relatively strong initial magnetizations. Most redbed specimens showed chemical changes at various temperatures. The temperatures at which chemical alteration caused increase in saturation magnetization ranged from 130°C to 400°C. Drastic changes in intensity continued at higher temperatures but decayed sharply around 570—580°C. This suggests that the newly produced magnetic mineral is probably magnetite (Curie temperature 578°C). Part of the saturation magnetization which remained unchanged up to 630°C was believed to reside on hematite. Chemical changes were also found for a specimen from site Ta02.

IRM acquisition

Text-fig. 7 shows the types of curves obtained during IRM acquisition experiments. Specimens representing non-red lithologies from Taltung Formation yielded curves presented in the upper diagram. With the exception of one specimen, all exhibit soft coercivities reflected in early saturation at fields around 0.1T attributable to (titano-) magnetite. Specimen Ta02-2D shows a curve in which positive slopes continue above 0.3T indicating the presence of higher coercivity mineral most probably hematite. This curve is, however, of composite nature as it clearly shows two distinct slopes. Strong magnitudes of IRM and the distinct lower portion suggests the presence of a substantial amount of magnetite as well. The relative magnitudes of IRM seem to be roughly proportional to initial NRM intensities and probably reflect the varying concentration of the magnetic minerals in these specimens.

IRM acquisition curves for redbeds are shown in Text-fig. 7b. Some of the heated specimens which exhibited significant chemical changes were studied in addition to fresh specimens. For fresh specimens, none of the curves presented shows saturation within the range of the applied field. This suggests to believe that hematite is the main

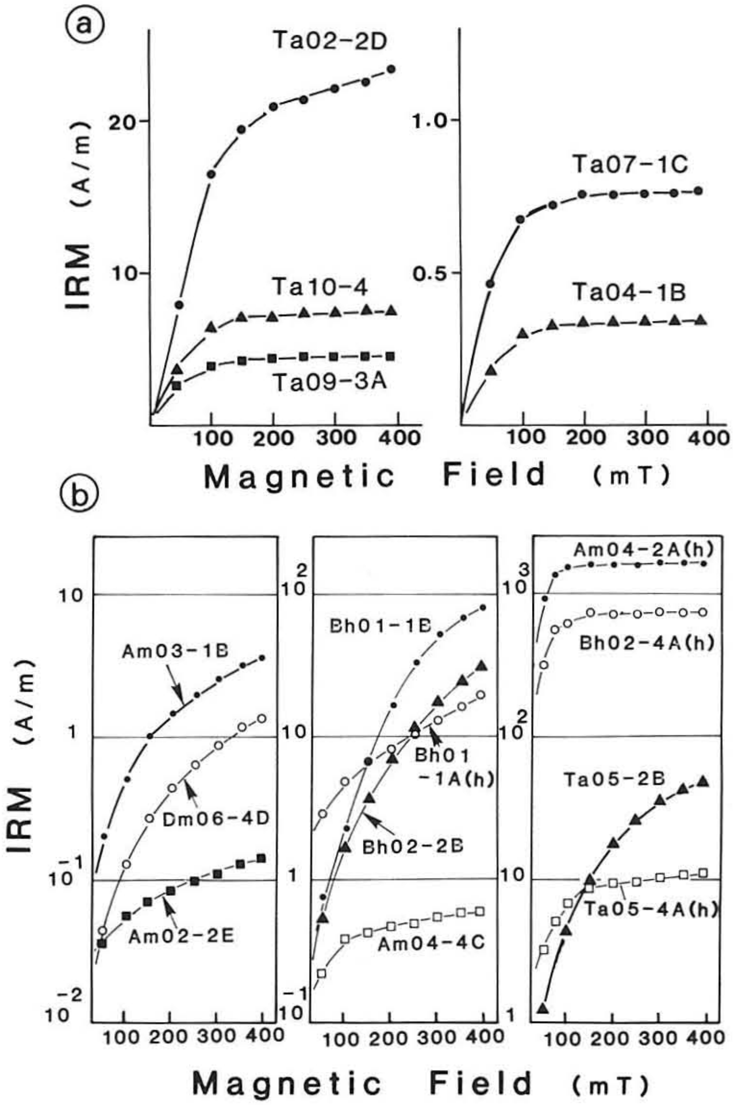

Text-fig. 7 Results of IRM acquisition experiments for some non-red specimens from Taltung Formation (a) and some redbed specimens (b). Specimens followed by (h) are heated at various temperatures, mostly above 500°C. Almost all heated specimens show early saturation (partial or complete) at fields, 0.1—0.2 T which is not shown by the unheated specimens.

magnetic constituent, although minor contribution of magnetite or maghemite cannot be denied specially in those specimens which attain significant portion of the IRM magnitudes at low fields. Among heated specimens, early saturation is attained in all but one (Bh01-1A(h)) with sharp increase in the IRM magnitudes. This suggests that heating caused formation of large amount of magnetite. The IRM curve for Bh01-1A(h)

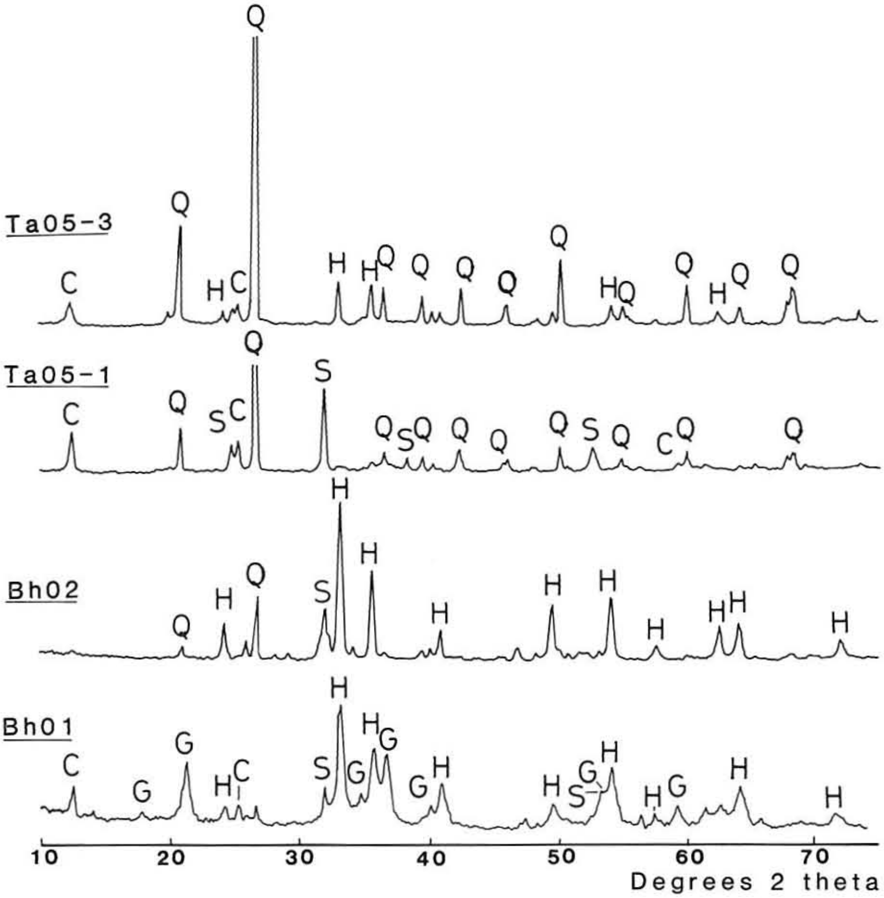

Text-fig. 8 X-ray powder diffraction patterns of some unheated redbed samples showing compositional variations. Q = quartz, H = hematite, S = siderite, G = goethite and C = chamosite.

has a shape which differs from that of the unheated specimens and has smaller magnitude. This curve indicates that hematite is the prominent mineral also in the heated specimens indicating that no severe chemical changes have occurred. The latter findings are consistent with the negligible chemical changes observed during thermal demagnetization.

X-ray analysis

X-ray diffraction patterns showing the variation in mineral phases in fresh and some heated chip specimens representing exclusively redbeds are shown in Text-figs. 8 and 9. Hematite, siderite, goethite and chamosite are the major iron-bearing phases present in varying proportions. In general, it was found that specimens which exhibited large-scale chemical changes during thermal demagnetization experiments are dominated by mineral siderite. A comparison of X-ray patterns obtained for unheated and heated samples (two chips from the same block sample were taken, one was crushed before heating and another after heating for X-ray measurements) as shown in the latter figure suggests that large amount of magnetite is formed in expense of initially contained siderite due to heating in the laboratory.

Laboratory chemical changes during heating: discussion

Laboratory chemical changes during heating red-colored sedimentary rocks or iron-ores has long been the object of interest in paleomagnetism. Instability of the rocks containing mineral siderite has been particularly noted. Seguin (1966) studied the rate of dissociation and instability of siderite ($FeCO_3$) in air over temperature range 25 to 300°C and found that siderite is capable to produce hematite (α-Fe_2O_3) as a solid-end product with transitional magnetite. He stressed that the rate of dissociation and oxidation of siderite is a function of grain size and temperature and the reactions may proceed quite rapidly for small crystals but take many thousand years for large crystals. Buchan and Hodych (1982), in a paleomagnetic study of the oolitic hematite beds of Ordovician age, found part of the samples containing siderite to exhibit dramatic increases in NRM intensities and random changes in directions. They observed that a strongly magnetic spinel phase with a Curie point of approximately 610°C was produced between 300 and 600°C of thermal treatment, with the interval 450—500°C being especially productive. After an analysis of possible contribution of various phases (chamosite, siderite, pyrite in addition to the dominant hematite) to form the new mineral, they concluded that thermal decomposition of siderite to "magnetite" was the most probable explanation. In a similar study, Ozdemir and Deutsch (1984) observed that their samples, also containing siderite and chamosite as secondary phases in addition to hematite as a major phase, showed dramatic increases in intensity and changes in direction in the range 400—600°C. They showed that large increases in intensity during heating were associated with high weight percentage of siderite and the new mineral produced in the expense of siderite during heating was magnetite as evidenced by X-ray diffraction patterns. In a more recent study, Ellwood et al. (1986) discuss the anomalous magnetic properties in siderite-bearing rocks and the possible paleomagnetic implication. They conclude that oxidation of siderite, a relatively non-magnetic iron mineral, can produce an intermediate but chemically unstable magnetic phase, maghemite (γ-Fe_2O_3), or magnetite, and finally a chemically stable phase of hematite. These oxidation effects include changes in susceptibility with time, self-reversals of the remanence, short-term viscous remagnetizations during sampling and laboratory storage period, and dramatic changes in anisotropy of magnetic susceptibility. Such changes are to be expected to occur in the rock when exposed to air due to erosion or quarrying or short-term exposures in air during field sampling or laboratory measurements. They hinted that development of an erosional disconformity may cause an oxidation leading to hematite production and hence remagnetization in it at low temperatures.

The present study reveals that siderite is a prominent constituent in the redbeds of

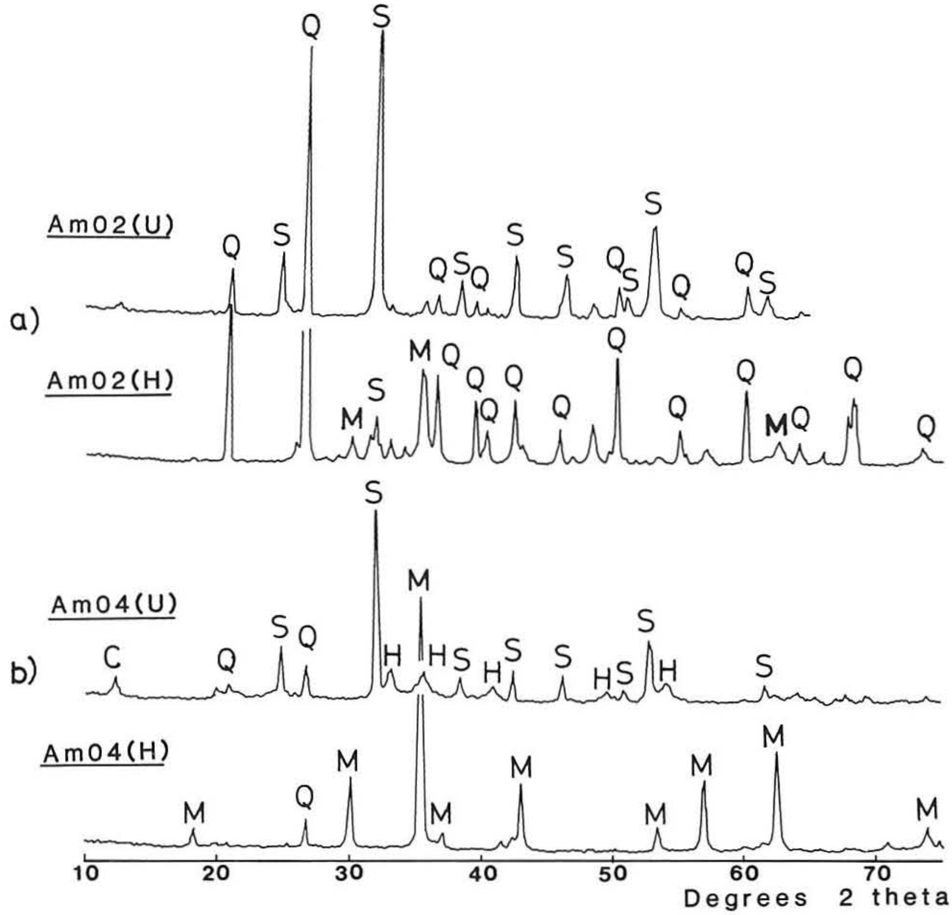

Text-fig. 9 Comparison of X-ray powder diffraction patterns of some unheated (U) and heated to 630°C (H) specimens. M is magnetite. Other symbols as before.

the Tansen area. Several lines of evidences obtained by independent experiments (Thermomagnetic analysis, IRM acquisition of unheated and heated siderite-bearing samples and X-ray analysis) confirm that this mineral when heated in the laboratory transforms to strongly magnetic phase of magnetite. Goethite, sometimes present, seems to carry a weak remanence. Intensity loss during initial steps of thermal demagnetization may probably be related to decomposition of goethite. In addition to this, some samples showed a sudden drop of a small fraction of intensity between temperature interval 200—300°C. According to Dekkers (1988) this is attributable to goethite-hematite conversion.

Directional analysis and discussion

Table 5 presents the summary of the directional analysis attempted on the basis of the data derived in this study and that from Aulis Volcanics (Gautam, 1989), which occur within the Taltung Formation. These data are displayed in equal area plots in Text-fig. 10.

Recognition of the primary or secondary nature of the components was primarily based on the degree of departure from the present dipole field at the sampling site and the orientation of the vectors, especially of inclination and their presence or absence in rocks of differing ages. Timing of the individual direction is primarily based on the comparison of the paleolatitude value derived from the mean inclination with the calculated paleolatitude pattern at Tansen (27.9°N, 83.5°E) expected from the simulated Indian Apparent Polar Wander Path (APWP) data for India (Klootwijk et al., 1985, Table 2C). This APWP covers a period of 80 Myr to 10 Myr B.P. Additional paleomagnetic data available in the literature (e.g., Klootwijk, 1984) were also consulted.

Component A, which represents the directions derived from demagnetization data at initial demagnetization steps, has a mean very close to the present dipole field ($I=47°$) at Tansen and obviously is of recent viscous origin. The directions with N to NNW declination and moderate downward inclinations forming component B are well grouped before any tilt corrections, are present in formations of varying ages and represent differing lithologies. These facts favor the secondary post-folding nature. The mean inclination yields 17°N paleolatitude which is to be expected in the area around 23 Myr (Early Miocene). The remanence resides in hematite in redbeds and in (titano-) maghemite in volcanics as shown by demagnetization behavior. This component postdates the major folding event in the region.

Two redbed sites Dm04 and Dm06 yield mean directions which are significantly different from the present field and also other components. The tilt-corrected mean directions are only 8° apart and their directions partially overlap suggesting that they can be regarded as drawn from a single population. So the mean direction was calculated combining all the tilt-corrected directions of 12 samples from two sites. The mean direction is interpreted to represent reverse polarity and acquired prior to folding. The high unblocking temperature remanence residing in hematite pigment is probably primary. The paleolatitude value of 9°N suggests its acquisition time to be around 40 Myr (Late Eocene). Site Am03 from Amile Formation yields a direction also of reverse polarity and yields a paleolatitude of 1°N placing it around 52 Myr (Early Eocene). The component, however, could not be completely free of the secondary components with high unblocking temperatures. A significant departure in declination with that of the Dumri Formation may partially be due to incomplete cleaning. The unblocking temperatures for this component are below 600°C and the probable carrier is hematite.

Component C is exclusively found to occur in Taltung Formation, both in sedimentary and volcanic rocks. The mean directions designed C2 in Table 3, which were based on peak field demagnetization approach, are combined with the C components from the volcanics. As is evident from the Table 5 and Text-fig. 10, the scatter in directions increases after tilt corrections. Due to this fact, it was suggested initially that this com-

Table 5 Summary of magnetic directions

Site(s): description	Mean Direction				VGP (north pole)				Paleolatitude (° N)
	D (deg.)	I (deg.)	k	α_{95} (deg.)	Lat. (° N)	long. (° E)	dp (deg.)	dm (deg.)	
1) **Characteristic (primary ?) directions:** (Corrected for bedding)									
a. Dm04 (4 samples)	143	−13	207	4.9					
b. Dm06 (8 samples)	141	−21	186	3.6					
a + b combined (12 samples)	143	−19	135	3.5	50	333	1	3	9
Am03 (7 samples)	191	−03	179	3.9	61	239	1	3	1
2) **Component A:** (*in situ*)									
AU1 (B), PG12, PG19, PG20, Ta09, Ta10 (6 sites)	003	47	133	4.9	87	157	4	6	28
3) **Component B:** (*in situ*)									
a. AU1 (B), PG12, PG19, PG20 (Volcanics: 4 sites)	339	32	44	10.5					
b. Ta04, Ta07, Ta09, Ta10 (Sediments: 4 sites)	349	28	37	11.6					
c. Bh01, Bh02, Am04 (Redbeds: 3 sites)	358	38	125	7.0					
a + b + c combined (11 sites)	347	32	39	6.8	74	314	4	7	17
4) **Component C:**									
a. Volcanics (*in situ*): AU12, PG12, PG14, PG19, PG20 (5 sites)	320	−50	24	12.8					
b. Sediments (*in situ*): Ta02, Ta04, Ta07 (3 sites)	339	−51	18	19.1					
a + b, combined:									
in situ (8 sites)	327	−50	22	10.6					
Bedding corrected (7 sites)	265	−67	11	15.8	−25	308	21	26	−50
5) **Component D:** (*in situ*)									
AU1 (B), PG12 (2 sites) (Reverse polarity)	171	54	—	—					

Note: Data from sites AU1, PG12, PG14, PG19, PG20 were taken from a separate study (Gautam, 1989). For other data refer Table 3 and Table 4. NRM direction from site Bh01 thought to represent the B component was also included.

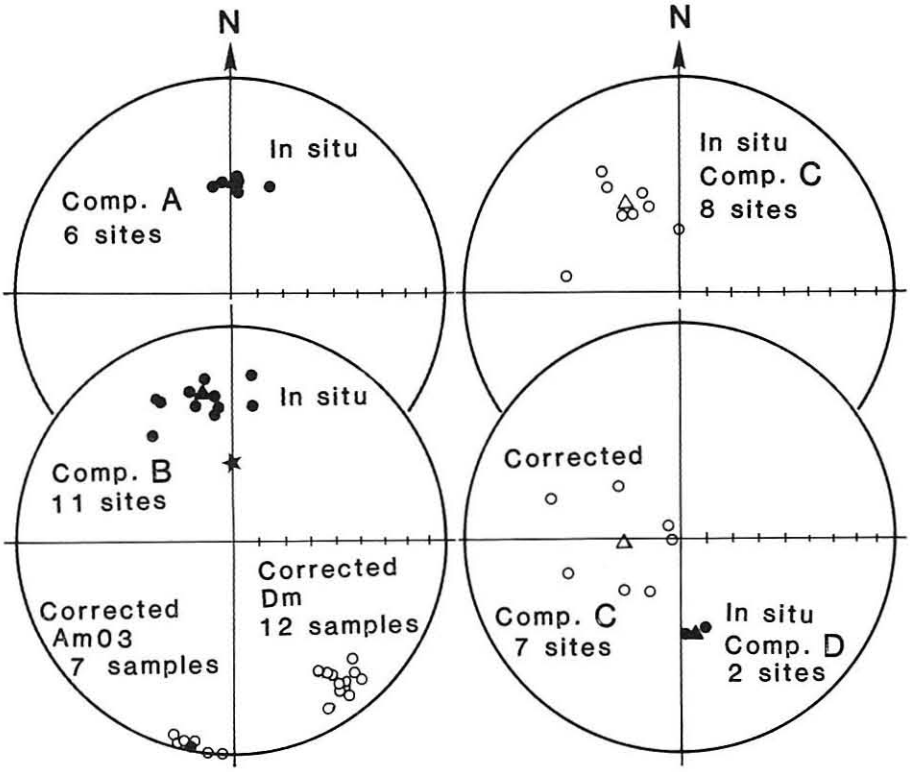

Text-fig. 10 Summary of the components/directions. Triangles represent mean directions. Star is the dipole field direction at Tansen. Plotting and other conventions as before.

ponent might be of secondary origin. The most probable paleolatitude of 32°S derived from the inclination of the uncorrected mean direction would have suggested an age of acquisition to be around 80 Myr. Such interpretation, however, contradicts with the assumption of the later folding of the region. Owing to this, the apparent worsening in grouping after bedding tilt-correction should probably be searched on other factors e.g. complex tectonism, imbrication structures, long or varying time span of the magnetization acquisition, etc. If the bedding corrected mean direction is considered as an approximation to the real one, the inclination ($I = -67°$) yields a very high paleolatitude of about 50°S. From two sites in the volcanics an another component designated as D, with reverse polarity, residing in Ti-poor magnetite could be estimated searching the convergence in remagnetization circles followed by data-points at higher TH demagnetization steps. This component had discrete unblocking temperatures very close to 550—560°C or above. Owing to the highest unblocking temperatures, this component is believed to have been acquired prior to the component C magnetization.

Sakai (1983) correlated the Aulis Volcanics with the Rajmahal/Bengal traps and the Taltung sedimentary rocks with the intertrappean sediments in the eastern part of Peninsular India. Recent K-Ar dating of those volcanics in eastern India by Baksi et al. (1987) indicates that the volcanic activity centered around 115 Myr ago. This estimate is slightly older than the generally accepted K-Ar age of 100—105 Myr for the Rajmahl traps in paleomagnetic literature (Klootwijk, 1984). Though the accurate estimation of the primary direction could not be achieved in this study, the occurence of the component C of normal polarity and the component D of reverse polarity may be of importance. In particular, it is possible that the component D was acquired during a period earlier than the Cretaceous long normal polarity epoch. The component C might have been acquired during the Cretaceous normal polarity epoch as is the case for the normal polarity paleomagnetic directions from the Rajmahal traps. This assumption, if proved to be correct by later studies, suggests the most probably age of Aulis volcanism to be around 118 Myr.

Conclusions

Main findings derived from the present study can be summarized as follows:

(1) Redbeds at various levels and olive green siltstone and sandstones possess strong magnetizations among the rocks of the Tansen Group. Many of the redbeds, however, consist of siderite which when heated in air even to moderate temperatures converts to magnetite. Thermal demagnetization is ineffective for the analysis of the stability of remanence in such siderite-bearing rocks.

(2) Apart from recent viscous remanence, the rocks exhibit magnetic components of various origin and ages. Magnetic directions of prefolding origin, probably primary depositional or acquired shortly after deposition, suggesting Late Eocene and Early Eocene were unraveled from Dumri and Amile Formations, respectively. Based on these data the age of the middle member of Dumri Formation is believed to be Late Eocene. A secondary component of post-folding origin acquired in Early Miocene time was found in rocks with varying lithologies. Directions with NW declinations and moderately upwards (-30 to $-60°$) inclinations are present in volcanics and sedimentary rocks of the Taltung Formation. In addition, presence of a reverse polarity component, approximately antipodal to the upward pointing direction mentioned was present in samples from some sites from the volcanics.

Acknowledgements

I would like to express sincere gratitudes to Dr. Y. Fujiwara for suggestions during the course of this study. Prof. M. Kato continuously encouraged and helped in various ways for which I am grateful. Discussions with Dr. H. Sakai, Dr. M. Yoshida and Dr. K. Arita, prior to the field work, were very useful. I would like to take this opportunity to express my sincere thanks to Dr. M.P. Sharma and Mr. M.R. Dhital for their encouragement and advices in various ways.

Receipt of the Japanese Monbusho (the Ministry of education and culture) research student scholarship is gratefully acknowledged.

References

Arita, K. and Yoshida, M., 1982. Geological observations along motor road from Butwal to Ramdighat, Central Nepal. *Jour. Nepal Geol. Soc.*, 2, Special issue: 51-58.

Bailey, R.C. and Halls, H.C., 1984. Estimate of confidence in paleomagnetic directions derived from mixed remagnetization circle and direct observational data. *J. Geophys.*, 54: 174-182.

Baksi, A.K., Barman, T.R., Paul, D.K. and Farrar, E., 1987. Widespread Early Cretaceous flood basalt volcanism in eastern India: Geochemical data from the Rajmahal-Bengal-Sylhet Traps. *Chem. Geol.*, 63: 133-141.

Buchan, K.L. and Hodych, J.P., 1982. Paleomagnetic reexamination of the Lower Ordovician Wabana and Bell Island Groups of the Avalon Peninsula of Newfoundland. *Can. J. Earth Sci.*, 19: 1055-1069.

Dekkers, M.J., 1988. Some rockmagnetic parameters for natural goethite, pyrrhotite and fine-grained hematite, Ph. D. thesis, University of Utrecht, *Geologica Utraiectina*, 51: 231 pp.

Dunlop, D.J., 1972. Magnetic mineralogy of unheated and heated red sediments by coercivity spectrum analysis. *Geophys. J.R. astr. Soc.*, 27: 37-55.

Ellwood, B.B., Balsam, W. and Burke, B., 1986. Anomalous magnetic properties in rocks containing the mineral siderite: paleomagnetic implications. *J. Geophys. Res.*, 91, B12: 12, 779-790.

Fuchs, G.R. and Frank, W., 1970. The Geology of West Nepal between the rivers Kali Gandaki and Thulo Bheri. *Jahrb. Geol. Bundesanst.*, 18: 103 pp.

Gautam, P., 1987. A paleomagnetic reconnaissance of some Late Precambrian to Early Paleozoic rocks of Tansen area, Lesser Himalaya, Nepal, *Jour. Fac. Sci., Hokkaido Univ., Ser.* IV, 22 (2): 259-275.

Gautam, P., 1989. Multicomponent remanent magnetization in the Aulis Volcanics, the Lesser Himalaya, Nepal. *J. Geomag. Geoelectr.*, 41: 101-117.

Hirayama, J., Nakajima, T., Shrestha, S.B., Adhikari, T.P., Tuladhar, R.M., Tamrakar, J.M. and Chitrakar G.R., 1988. Geology of the southern part of the Lesser Himalaya, West Nepal, *Bull. Geol. Surv. Japan.*, vol. 39 (4): 205-249.

Kirschvink, J.L., 1980. The least-squares line and plane and the analysis of palaeomagnetic data, *Geophys. J.R. astr. Soc.*, 62: 699-718.

Klootwijk, C.T., 1984. A review of Indian Phanerozoic paleomagnetism: Implications for the India-Asia collision. *Tectonophysics*, 105: 331-353.

Klootwijk, C.T., P.J. Conaghan and C. McA. Powell, 1985. The Himalayan Arc: large-scale continental subduction, oroclinal bending and back-arc spreading, *Earth and Planet Sci. Lett.*, 75: 167-183.

Ozdemir, O. and Deutsch, E.R., 1984. Magnetic properties of oolitic iron ore on Bell island, Newfoundland. *Earth and Planet. Sci. Lett.*, 69: 427-441.

Sakai, H., 1983. Geology of the Tansen Group of the Lesser Himalaya in Nepal, *Mem. Fac. Sci., Kyushu Univ.*, ser. D, Geol., xxv (1): 27-74.

Schmidt, P.W., 1982. Linearity spectrum analysis of multi-component magnetization and its application to some igneous rocks from south-eastern Australia. *Geophys. J.R. astr. Soc.*, 70: 647-665.

Seguin, M., 1966. Instability of $FeCO_3$ in air. *Am. J. Science*, 264: 562-568.

Sharma, T., Kansakar, D.R. and Kizaki, K., 1984. Geology and Tectonics of the region between Kali Gandaki and Bheri rivers in Central West Nepal. *Bull. College of Science, Univ. of the Ryukyus*, 38: 57-102.

Yoshida, M. and Sakai, H., 1984. Some observations on the Paleomagnetism of Tansen Group, West Central Nepal, *Jour. Nepal Geol. Soc.*, 4, Special issue: 53-61.

Zijderveld J.D.A., 1967. A.C. demagnetization of rocks: analysis of results. In: D.W. Collinson, K.M. Creer and S.K. Runcorn (Editors), *Methods in Paleomagnetism.*, Elsevier, Amsterdam: 254-286.

(Manuscript received on Oct. 28, 1988; and accepted on Nov. 30, 1988)